

WATER VAPOR FEEDBACK AND GLOBAL WARMING¹

Isaac M. Held and Brian J. Soden

Geophysical Fluid Dynamics Laboratory/National Oceanic and Atmospheric Administration, Princeton, New Jersey 08542

Key Words climate change, climate modeling, radiation

■ **Abstract** Water vapor is the dominant greenhouse gas, the most important gaseous source of infrared opacity in the atmosphere. As the concentrations of other greenhouse gases, particularly carbon dioxide, increase because of human activity, it is centrally important to predict how the water vapor distribution will be affected. To the extent that water vapor concentrations increase in a warmer world, the climatic effects of the other greenhouse gases will be amplified. Models of the Earth's climate indicate that this is an important positive feedback that increases the sensitivity of surface temperatures to carbon dioxide by nearly a factor of two when considered in isolation from other feedbacks, and possibly by as much as a factor of three or more when interactions with other feedbacks are considered. Critics of this consensus have attempted to provide reasons why modeling results are overestimating the strength of this feedback.

Our uncertainty concerning climate sensitivity is disturbing. The range most often quoted for the equilibrium global mean surface temperature response to a doubling of CO₂ concentrations in the atmosphere is 1.5°C to 4.5°C. If the Earth lies near the upper bound of this sensitivity range, climate changes in the twenty-first century will be profound. The range in sensitivity is primarily due to differing assumptions about how the Earth's cloud distribution is maintained; all the models on which these estimates are based possess strong water vapor feedback. If this feedback is, in fact, substantially weaker than predicted in current models, sensitivities in the upper half of this range would be much less likely, a conclusion that would clearly have important policy implications. In this review, we describe the background behind the prevailing view on water vapor feedback and some of the arguments raised by its critics, and attempt to explain why these arguments have not modified the consensus within the climate research community.

CONTENTS

HISTORICAL INTRODUCTION TO THE BASIC PHYSICS	442
The Greenhouse Effect and the Radiative Properties of Water Vapor	442

¹The US Government has the right to retain a nonexclusive, royalty-free license in and to any copyright covering this paper.

Early Studies of Climatic Sensitivity	443
Radiative-Convective Models	445
Energy Balance	446
The Satellite Era	449
Climate Models	452
The Simplest Feedback Analysis	454
THE CLIMATOLOGICAL RELATIVE HUMIDITY DISTRIBUTION	456
The Global Picture	456
The Planetary Boundary Layer	459
The Free Troposphere	460
RELATIVE IMPORTANCE OF DIFFERENT PARTS OF THE TROPOSPHERE FOR WATER VAPOR FEEDBACK	461
THE CONTROVERSY CONCERNING WATER IN THE TROPICAL FREE TROPOSPHERE	465
The Complexity of the Tropics	465
Convective Outflow Temperatures	466
Condensate	468
Precipitation Efficiency	468
Empirical Studies	469
FINAL REMARKS	471

HISTORICAL INTRODUCTION TO THE BASIC PHYSICS

The Greenhouse Effect and the Radiative Properties of Water Vapor

Joseph Fourier is widely credited as being the first to recognize the importance of the greenhouse effect for the Earth's climate. In his 1827 treatise on the temperature of the globe, Fourier pointed out that the atmosphere is relatively transparent to solar radiation, but highly absorbent to thermal radiation and that this preferential trapping is responsible for raising the temperature of the Earth's surface (1). By 1861, John Tyndal had discovered that the primary contributors to this trapping are not the dominant constituents of the atmosphere, N_2 and O_2 , but trace gases, particularly water vapor and carbon dioxide, which constitute less than 1% of the atmospheric mass (2). From a series of detailed laboratory experiments, Tyndal correctly deduced that water vapor is the dominant gaseous absorber of infrared radiation, serving as "a blanket, more necessary to the vegetable life of England than clothing is to man" (3).

The development of quantum theory in the early twentieth century and improved spectroscopic measurements rapidly produced a more detailed understanding of the interactions between atmospheric gases and radiation. The qualitative picture first painted by Fourier and Tyndal has, of course, been confirmed and refined. The wavelength-dependence of the absorption in the atmosphere is rich in detail, consisting of thousands of spectral lines for water vapor alone. One might suspect that this complexity of the radiative transfer is itself an important source of

uncertainty in estimates of climate sensitivity, but this is true only to a very limited degree.

The major source of uncertainty in gaseous radiative transfer arises from the continuum absorption by water vapor (4, 5). Far from any line centers, there remains background absorption due to the far wings of distant spectral lines. Knowledge of the precise shape of these lines is incomplete. Line shapes in the troposphere are primarily controlled by pressure broadening, implying that most of the interactions with radiation occur while the radiatively active gas molecule is colliding with another molecule. The water vapor continuum is distinctive in that it is controlled in large part by collisions of water molecules with other water molecules, and it therefore plays an especially large role in the tropics, where water vapor concentrations are highest. Continuum absorption is quantitatively important in computations of the sensitivity of the infrared flux escaping the atmosphere to water vapor concentrations within the tropics (6), a centrally important factor in analyses of water vapor feedback. However, approximations for continuum absorption are constrained by laboratory and atmospheric measurements and the remaining uncertainty is unlikely to modify climatic sensitivity significantly.

There is also room for improvement in the construction of broadband radiation algorithms for use in climate models that mimic line-by-line calculations (7), but work growing out of the Intercomparison of Radiation Codes for Climate Models project (8) has helped to reduce the errors in such broadband computations. In short, we see little evidence to suggest that our ability to estimate climate sensitivity is significantly compromised by errors in computing gaseous absorption and emission, assuming that we have accurate knowledge of the atmospheric composition.

There does remain considerable controversy regarding the radiative treatment of clouds in climate models, associated with the difficulty in obtaining quantitative agreement between atmospheric measurements and theoretical calculations of solar absorption in cloudy atmospheres (9). As we shall see below, the treatment of clouds in climate models presents greater obstacles to quantitative analysis of climate sensitivity than does the treatment of water vapor.

Early Studies of Climatic Sensitivity

By the turn of the century, the possibility that variations in CO_2 , could alter the Earth's climate was under serious consideration, with both S Arrhenius (10) and TC Chamberlin (11) clearly recognizing the central importance of water vapor feedback. In a letter to CG Abbott in 1905, Chamberlin writes,

[W]ater vapor, confessedly the greatest thermal absorbent in the atmosphere, is dependent on temperature for its amount, and if another agent, as CO_2 , not so dependent, raises the temperature of the surface, it calls into function a certain amount of water vapor which further absorbs heat, raises the temperature and calls forth more vapor ... (3).

In the following, we will measure the concentration of water vapor either by its partial pressure e or its mixing ratio r , the latter being the ratio of the mass of

water vapor in a parcel to the mass of dry air. Since observed mixing ratios are small, we can assume that $r \propto e/p$, where p is the atmospheric pressure. If there are no sources or sinks of water, r is conserved as the parcel is transported by the atmospheric flow.

As understood by Chamberlin, when air containing water vapor is in thermodynamic equilibrium with liquid water, the partial pressure of the vapor, e , is constrained to equal $e_s(T)$, the saturation vapor pressure, which is a function of the temperature T only (ignoring impurities in the water and assuming a flat liquid surface). The ratio $H \equiv e/e_s$ is referred to as the relative humidity. Supersaturation of a few percent does occur in the atmosphere, especially when there is a shortage of condensation nuclei on which drops can form, but for large-scale climate studies it is an excellent approximation to assume that whenever e rises above e_s vapor condenses to bring the relative humidity back to unity. In much of the atmosphere it is the saturation pressure over ice, rather than water, that is relevant, but we will not refer explicitly to this distinction.

According to the Clausius-Clapeyron relation, $e_s(T)$ increases rapidly with increasing temperature, albeit a bit slower than exponentially. More precisely, the fractional change in e_s resulting from a small change in temperature is proportional to T^{-2} . At 200 K, a 1 K increase results in a 15% increase in the vapor pressure; at 300 K, it causes a 6% increase. In searching for theories for the ice-ages, Arrhenius and Chamberlin both thought it plausible, if not self-evident, that warming the atmosphere by increasing CO_2 would, by elevating e_s , cause water vapor concentrations to increase, which would further increase the greenhouse effect, amplifying the initial warming.

The possibility of CO_2 increasing because of fossil fuel use helped motivate a series of studies through the 1930s, 1940s, and 1950s that improved the radiative computations underlying estimates of climate sensitivity (12–14). Researchers evidently lost sight of the potential importance of water vapor feedback during this period. In 1963 F Moller (15) helped correct this situation, from which time this issue has retained center stage in all quantitative studies of global warming. At roughly the same time, a runaway greenhouse owing, at least in part, to water vapor began to be considered as having possibly occurred during the evolution of the Venusian atmosphere (16).

In his attempt at quantifying the strength of water vapor feedback, Moller explicitly assumed that the relative humidity of the atmosphere remains fixed as it is warmed. This assumption of fixed relative humidity has proven to be a simple and useful reference point for discussions of water vapor feedback. The alternative assumption of fixed vapor pressure requires that relative humidity H decrease rapidly as temperatures increase, the decrease being 6% of H per $^\circ\text{C}$ of warming in the warmest parts of the troposphere, and 15% of H per $^\circ\text{C}$ in its coldest parts.

The relative humidity is controlled by the atmospheric circulation. Motion dries the atmosphere by creating precipitation. For example, as air moves upwards it cools due to adiabatic expansion. The vapor pressure e decreases due to this expansion, but e_s decreases much more rapidly, causing the vapor to condense.

Once sufficient condensate is generated, raindrops form and water falls out of the parcel. When restored to its original level the air parcel compresses and warms, and once again the change in e_s far outweighs the increase in vapor pressure due to the compression itself, and the parcel finds itself undersaturated.

To model the relative humidity distribution and its response to global warming one requires a model of the atmospheric circulation. The complexity of the circulation makes it difficult to provide compelling intuitive arguments for how the relative humidity will change. As discussed below, computer models that attempt to capture some of this complexity predict that the relative humidity distribution is largely insensitive to changes in climate.

Radiative-Convective Models

When Moller assumed fixed relative humidity in a one-dimensional atmospheric model, he found an implausibly large sensitivity to changes in CO_2 . His results were in error owing to a focus on the radiative fluxes at the surface, rather than at the top of the atmosphere. The atmosphere is not in pure radiative equilibrium; in fact, the vertical and horizontal temperature structure within the troposphere is strongly controlled by the atmospheric circulation as well as by the spatial structure of the radiative fluxes. The sensitivity of surface temperature is more closely tied to changes in the radiative fluxes at the top of the atmosphere or more precisely, at the tropopause, than at the surface. S Manabe and collaborators (17, 18), working with simple one-dimensional radiative-convective models in the 1960s, helped clarify this centrally important point.

On average, temperatures in the troposphere decrease with height at a rate (the lapse rate) of 6.5 K/km. This vertical temperature structure cannot be understood from consideration of radiative equilibrium alone, which would produce a much larger lapse rate. Rather, it is primarily controlled by the atmospheric circulation. In those areas of the tropics that are convectively active, the lapse rate is close to that of a moist adiabat, the profile obtained by raising a saturated parcel, which cools owing to adiabatic expansion, but as a result of this cooling also condenses water vapor, releasing the latent heat of evaporation that compensates for part of the cooling. At higher latitudes, the moist adiabat does not provide as useful an approximation to the lapse rate, as the sensible and latent heat transport by larger scale circulations, extratropical cyclones, and anticyclones also plays a significant role. Models for the nonradiative fluxes of energy in the atmosphere are inherently complex. Different processes are dominant in different regions, and a variety of scales of motion are involved.

Manabe and collaborators (17, 18) introduced a very simple, approximate way of circumventing this complexity, by starting with a one-dimensional radiative-equilibrium model of the horizontally-averaged temperature of the atmosphere but then adding the constraint that the lapse rate should not be allowed to rise above some prescribed value. The model then predicts the position of the tropopause, below which it is forced to maintain the prescribed lapse rate, and above which

it maintains pure radiative equilibrium. Nonradiative fluxes are implicit in the upward energy flux required to maintain the tropospheric lapse rate.

In the simplest radiative-convective models, one also sets the temperature of the surface equal to the temperature of the atmosphere adjacent to the surface. In pure radiative equilibrium there is a substantial temperature jump at the surface. The removal of this jump implies that there is evaporation or sensible heat flux at the surface, determined by the radiative flux imbalance. Changes in the net radiation at the surface are assumed to be perfectly compensated by changes in the evaporation and the surface sensible heat flux. In contrast, Moller had effectively assumed, as had others before him, that the surface temperature would adjust to any changes in radiative fluxes, holding evaporation and sensible heating fixed. Because the latter are very strongly dependent on the temperature difference between the surface and the lowest layers of the atmosphere, one is much better off assuming that the surface fluxes adjust as needed to remove this temperature difference. To the extent that evaporation dominates over the surface-sensible heat flux, one can, in fact, argue that changes in the net radiation at the surface control the sensitivity of the global hydrologic cycle (the mean rate of precipitation or evaporation) rather than the sensitivity of surface temperatures.

It is an oversimplification to assume that temperature gradients within the troposphere do not change as the climate warms, but this simple assumption has proven to be a very useful point of reference. Using a radiative convective model constrained in this way, and with the additional assumption that the relative humidity is fixed, Manabe & Wetherald (18) found that the sensitivity of surface (and tropospheric) temperatures to CO_2 is increased by a factor of ≈ 1.7 over that obtained with fixed water vapor. Other radiative-convective models have supported this estimate of the strength of water vapor feedback, with fixed relative humidity, fixed clouds, and fixed lapse rate, rarely varying by more than 10% from this value. For further information on radiative-convective models, see Ramanathan & Coakley (19).

Energy Balance

The simple radiative-convective framework teaches us to think of the energy balance of the Earth as a whole as the starting point for discussions of climate sensitivity.

Averaged over the surface and over the seasons, the Earth absorbs $\approx 70\%$ of the solar radiation incident at the top of the atmosphere, amounting to $\approx 240 \text{ W/m}^2$. To balance this incoming flux, a black body would have to radiate to space at a temperature of 255 K. We refer to this temperature as the effective temperature of the infrared emission, T_e . We have $S = \sigma T_e^4$, where S is the absorbed solar flux and σ is the Stefan-Boltzmann constant. The actual mean surface temperature of the Earth is close to 288 K. The effective temperature of emission occurs in the mid-troposphere, about 5 km above the surface on average. We refer to this height as Z_e . As pictured in Figure 1, one can think of the average infrared photon escaping to space as originating near this mid-tropospheric level. Most photons

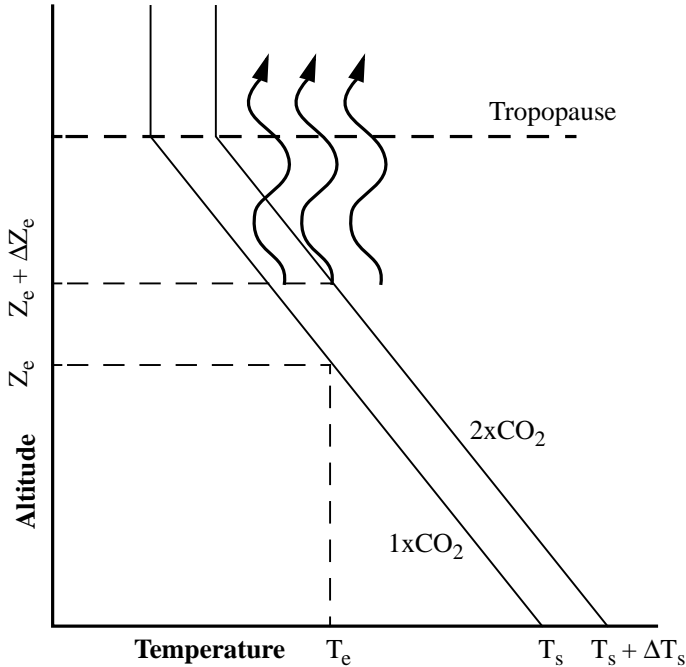


Figure 1 Schematic illustration of the change in emission level (Z_e) associated with an increase in surface temperature (T_s) due to a doubling of CO_2 assuming a fixed atmospheric lapse rate. Note that the effective emission temperature (T_e) remains unchanged.

emitted from lower in the atmosphere, including most of those emitted from the surface, are absorbed by infrared-active gases or clouds and are unable to escape directly to space. The surface temperature is then simply $T_s = T_e + \Gamma Z_e$, where Γ is the lapse rate. From this simple perspective, it is the changes in Z_e , as well as in the absorbed solar flux and possibly in Γ , that we need to predict when we perturb the climate. As infrared absorbers increase in concentration, Z_e increases, and T_s increases proportionally if Γ and S remain unchanged.

The increase in opacity due to a doubling of CO_2 causes Z_e to rise by ≈ 150 meters. This results in a reduction in the effective temperature of the emission across the tropopause by $\approx (6.5 \text{ K/km}) (150 \text{ m}) \approx 1 \text{ K}$, which converts to 4 W/m^2 using the Stefan-Boltzmann law. This radiative flux perturbation is proportional to the logarithm of the CO_2 concentration over the range of CO_2 levels of relevance to the global warming problem. Temperatures must increase by $\approx 1 \text{ K}$ to bring the system back to an equilibrium between the absorbed solar flux and the infrared flux escaping to space (Figure 1). In radiative-convective models with fixed relative humidity, the increase in water vapor causes the effective level of emission to move upwards by an additional $\approx 100 \text{ m}$ for a doubling of CO_2 . Water vapor also absorbs solar radiation in the near infrared, which feeds back with the same sign as the

terrestrial radiation component, accounting for $\approx 15\%$ of the water vapor feedback in climate models (20, 21).

In equilibrium, there is a balance between the absorbed solar flux S and the outgoing terrestrial radiation R . Listing a few of the parameters on which these fluxes depend, we have, schematically,

$$S(H_2O, I, C) = R(T, H_2O, \log_2 CO_2, C), \tag{1}$$

where C represents clouds, I the ice and snow cover, $\log_2 CO_2$ is the logarithm of the CO_2 concentration (base 2) and T is either the mean surface temperature or a mean tropospheric temperature (we are assuming here that these temperatures all change uniformly). Perturbing CO_2 and holding H_2O , I , and C fixed, the perturbation in temperature dT satisfies

$$0 = \frac{\partial R}{\partial T} dT + \frac{\partial R}{\partial \log_2 CO_2} d\log_2 CO_2 \tag{2}$$

Linearizing about the present climate, we can summarize the preceding discussion by setting

$$\frac{\partial R}{\partial T} \approx 4 \text{ W}/(\text{m}^2\text{K}) \tag{3}$$

and

$$\frac{\partial R}{\partial \log_2 CO_2} \approx -4 \text{ W}/\text{m}^2 \tag{4}$$

so that

$$\frac{dT}{d\log_2 CO_2} = -\frac{\partial R}{\partial \log_2 CO_2} / \frac{\partial R}{\partial T} \equiv \Delta_0 \approx 1 \text{ K} \tag{5}$$

for fixed H_2O , C , and I .

If we believe that changes in water vapor are constrained by changes in atmospheric temperature, we can set $H_2O = H_2O(T)$. Replacing equation 2, we have

$$\frac{\partial S}{\partial H_2O} \frac{dH_2O}{dT} dT = \frac{\partial R}{\partial T} dT + \frac{\partial R}{\partial H_2O} \frac{dH_2O}{dT} dT + \frac{\partial R}{\partial \log_2 CO_2} d\log_2 CO_2 \tag{6}$$

The temperature response to CO_2 doubling is now

$$\frac{dT}{d\log_2 CO_2} = \frac{\Delta_0}{1 - \beta_{H_2O}}, \tag{7}$$

where

$$\beta_{H_2O} \equiv \left(-\frac{\partial R}{\partial H_2O} + \frac{\partial S}{\partial H_2O} \right) \frac{dH_2O}{dT} / \frac{\partial R}{\partial T}. \tag{8}$$

The size of nondimensional ratio, β_{H_2O} , provides a measure of the strength of the water vapor feedback. If $\beta_{H_2O} \approx 0.4$, water vapor feedback increases the sensitivity of temperatures to CO_2 by a factor of ≈ 1.7 , assuming that I and C are fixed.

If the value of β_{H_2O} were larger than unity, the result would be a runaway greenhouse. The outgoing infrared flux would decrease with increasing temperatures. It is, of course, self-evident that the Earth is not in a runaway configuration. But it is sobering to realize that it is only after detailed computations with a realistic model of radiative transfer that we obtain the estimate $\beta_{H_2O} \approx 0.4$ (for fixed relative humidity). There is no simple physical argument of which we are aware from which one could have concluded beforehand that β_{H_2O} was less than unity. The value of β_{H_2O} does, in fact, increase as the climate warms if the relative humidity is fixed. On this basis, one might expect runaway conditions to develop eventually if the climate warms sufficiently. Although it is difficult to be quantitative, primarily because of uncertainties in cloud prediction, it is clear that this point is only achieved for temperatures that are far warmer than any relevant for the global warming debate (22).

The Satellite Era

Given that the earth's climate is strongly constrained by the balance between the absorption of solar radiation and emission of terrestrial radiation, space-based observations of this radiation budget play a centrally important role in climate studies. These observations first became available in the mid-1960s. After two decades of progress in satellite instrumentation, a coordinated network of satellites [the Earth Radiation Budget Experiment (ERBE)] was launched in 1984 to provide comprehensive measurements of the flow of radiative energy at the top of the atmosphere (23). Over a century after John Tyndal first noted its importance, an observational assessment of our understanding of the radiative trapping by water vapor became possible.

When analyzing the satellite measurements, it has proven to be particularly valuable to focus on the outgoing longwave fluxes when skies are free of clouds, R_{clear} , to highlight the effects of water vapor. Following Raval & Ramanathan (24), in Figure 2a (see color insert) we use ERBE observations to plot the annual mean clear sky greenhouse effect, $G_{clear} \equiv R_s - R_{clear}$ over the oceans, where R_s is the longwave radiation emitted by the surface. (In the infrared, ocean surfaces emit very nearly as black bodies, so that R_s is simply σT_s^4 .) A simple inspection of these figures reveals several important features regarding the processes that control the atmospheric greenhouse effect.

The magnitude of greenhouse trapping is largest over the tropics and decreases steadily as one approaches the poles. Moreover, the distribution of the clear-sky greenhouse effect closely resembles that of the vertically-integrated atmospheric water vapor (Figure 2b; see color insert). The thermodynamic regulation of this column-integrated vapor is evident when comparing this distribution with that of

surface temperature (Figure 2c; see color insert). Warmer surface temperatures are associated with higher water vapor concentrations, which in turn, are associated with a larger greenhouse effect. Regressing G_{clear} versus T_s over the global oceans (24, 25), one finds a relationship that is strikingly similar to that obtained from radiative computations assuming clear sky, fixed lapse rate, and fixed relative humidity.

Such an analysis suggests the tantalizing possibility that the strength of water vapor feedback might be determined directly from observations rather than relying upon models. Unfortunately, life is not so simple. The vapor distribution in Figure 2 is not solely a function of surface temperature. Even if the relative humidity were fixed, variations in atmospheric temperature do not always follow surface temperature changes in a simple way. For example, the relationship between R_{clear} and T_s obtained from geographic variations in mid-latitudes differs markedly from those obtained from the local seasonal cycle, owing to differences in the variations in lapse rate; similarly, the relation observed on seasonal time scales differs markedly from that observed on interannual time scales (26).

More importantly still, the relative humidity distribution is strongly affected by the atmospheric circulation, with areas of mean ascent moister than areas of mean subsidence. Over the tropical oceans, in particular, ascent occurs in the regions of warmest surface temperature, and strong descent occurs in regions where the surface is only a few degrees cooler. The circulation can be thought of as forced, in first approximation, by the difference in surface temperature between these two regions, not by the absolute temperature itself. Let us suppose that the atmosphere warms uniformly and that the circulation does not change. Schematically, we can set $R = R(T, \omega)$ where ω is the vertical motion. A simple regression of R with T in the tropics that does not take into account that ω is spatially correlated with T incorrectly suggests the existence of a “super-greenhouse effect” (27).

One attempt to avoid this circulation dependence is exemplified by Soden (28), who averaged over the ascending and descending regions of the tropics and used interannual variations produced by El Niño as the source of variability. Figure 3 shows the evolution of G_{clear} averaged over the tropics for a 4-year period containing the El Niño event in 1988. An increase in tropical-mean greenhouse trapping of $\approx 2\text{W/m}^2$ is observed in conjunction with a $\approx 0.4\text{ K}$ increase in tropical-mean sea surface temperature. These tropical mean results are the small difference between larger regional changes that are dominated by the dramatic changes in the pattern of ascent and descent that occur during El Niño. There is no reason to believe that global warming will be accompanied by similar circulation changes. One can conceive of a number of ways in which the regional changes might be nonlinearly rectified to produce a tropical mean infrared trapping that is different in El Niño warming and CO_2 -induced warming. Indeed, at face value, the results in Figure 3 suggest a value of $\beta_{\text{H}_2\text{O}}$ much larger than 0.4.

In recent years, efforts along these lines have been redirected away from attempts at obtaining direct empirical estimates of climate sensitivity, and towards providing a record of variability against which model predictions may be tested. As an example, Figure 3 also shows the prediction of a climate model (one

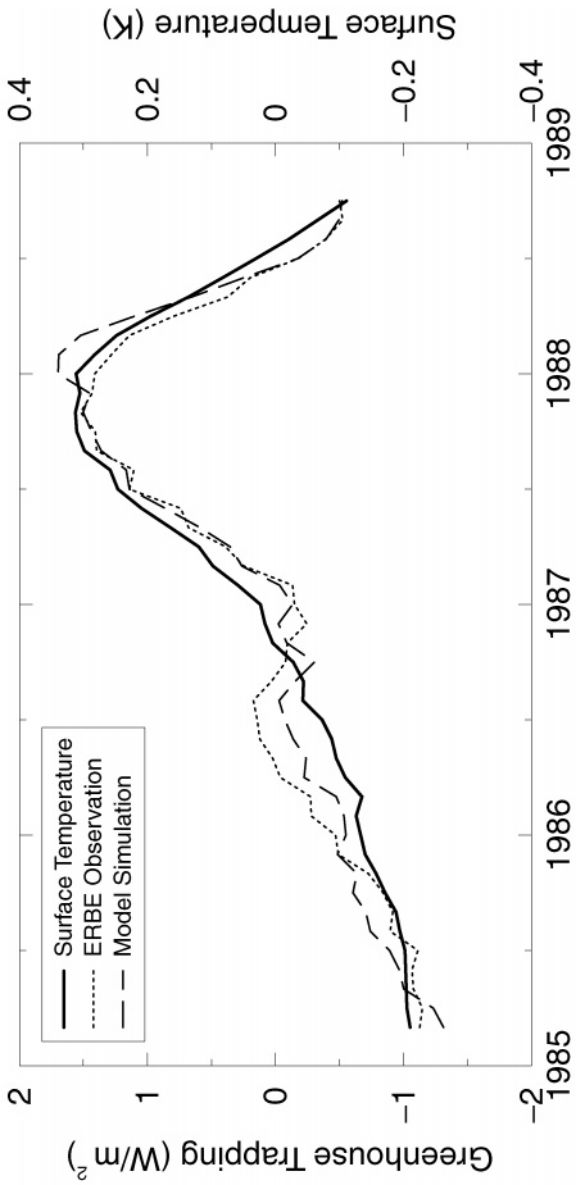


Figure 3 A time series of the tropical-mean interannual anomalies in clear-sky greenhouse trapping (G_{clear}) for 1985–1988 from ERBE (Earth Radiation Budget Experiment) observations (*dashed line*) and GFDL (Geophysical Fluid Dynamics Laboratory) model simulations (*dotted line*). For reference, the tropical-mean anomalies in sea surface temperature are also shown (*thick line*).

constructed at National Oceanic and Atmospheric Administration's Geophysical Fluid Dynamics Laboratory), when the observed sea surface temperatures are used as a surface boundary condition. The model simulates the variations in clear-sky infrared trapping very well, although studies of longer data sets suggest that the response of the moisture field, and the ability of climate models to reproduce the observed response, may differ from one El Niño event to the next (29). One also finds that the model does less well at simulating the observed variations in the net outgoing radiation (solar plus terrestrial, including cloudy as well as clear skies), once again strongly suggesting that the prediction of clouds and their radiative properties are the central difficulty facing the model, not water vapor.

Empirical studies such as that in Figure 3 do not provide a direct proxy for CO₂-included warming. Rather, the degree of similarity between the observed and modeled response of G_{clear} to changes in surface temperature provides a measure of confidence in the ability of the climate model to accurately represent the relevant physical processes involved in determining G_{clear} , and therefore to correctly predict the water vapor feedback that would occur under various global warming scenarios. Our dependence on models is unavoidable when analyzing a system as complex as that maintaining our climate.

Climate Models

The idea of predicting the weather by integrating the equations governing the atmospheric state forward in time was made explicit by V Bjerknes (30) in 1904. LF Richardson (31) made the first serious, but famously unsuccessful, attempt at gathering data to provide an initial condition and actually integrating a version of these equations. At the dawn of the computer age, J von Neumann, J Charney, and others realized that the resulting computational power would make numerical weather prediction feasible. The success of this enterprise has been impressive (32). Predictions of the atmospheric state for up to 10 days in advance continue to improve, and the meteorological services of the world continue to be prime customers of the largest supercomputers in existence, as more computer power translates into better forecasts.

Building on this effort in weather prediction, through the 1960s and 1970s a parallel effort began toward the development of numerical models of the Earth's climate. In climate modeling, the emphasis shifts to the long-term statistics of the atmospheric (as well as oceanic and cryospheric) state, and the sensitivity of these statistics to perturbations in external parameters, rather than the short-term evolution from particular initial conditions. Because they are integrated over longer periods, the spatial resolution of climate models is always lower than that of state-of-the-art weather prediction models. In the past few years global warming scenarios have typically been generated using atmospheric models with effective grid sizes of roughly 200–300 kms, with ≈ 10 vertical levels within the troposphere. An order of magnitude increase in computer power allows roughly a factor of two decrease in the effective grid size. Climate warming

scenarios with horizontal atmospheric resolution of 100 km and less will become available in the next few years. Much more ambitious plans are being laid. For example, the Japanese frontier Research System for Global Change (<http://www.frontier.esto.or.jp>) has the goal of constructing a global climate model with 10 km resolution.

There is a large gap between climate sensitivity experiments with comprehensive climate models and computations with simple models like the radiative-convective model. Because of the turbulent character of atmospheric flows, the complex manner in which the atmosphere is heated (through latent heat release and by radiative fluxes modified by intricate cloud distributions) as well as the rather complex boundary condition that the Earth's surface provides, it has proven difficult to develop models of an intermediate complexity to fill this gap, and the continuing existence of the gap colors the sociology of the science of global warming. Building and analyzing climate models is an enterprise conducted by a small number of groups with substantial computational resources.

Many processes occur in the atmosphere and oceans on scales smaller than those resolved by these models. These scales of motion cannot simply be ignored; rather, the effects of these small scales on larger scales must be approximated to generate a meaningful climate. Some aspects of this closure problem have been reasonably successful, whereas others are ad hoc or are based on empirical relations that may not be adequate for understanding climate change. Skeptics focus on these limitations. For a balanced view, it is useful to watch an animation of the output of such a model, starting from an isothermal state of rest with no water vapor in the atmosphere and then "turning on the sun," seeing the jet stream develop and spin off cyclones and anticyclones with statistics that closely resemble those observed, watching the Southeast Asian monsoon form in the summer, and in more recent models, seeing El Niño events develop spontaneously in the Pacific Ocean.

The first results of the sensitivity of such a climate model to an increase in CO₂ were presented in 1975 by Manabe & Wetherald (33) with an atmosphere-only model over an idealized surface with no heat capacity, no seasonal cycle, and with fixed cloud cover. The equilibrium sensitivity of global mean surface temperature obtained was ≈ 3 K for a doubling of CO₂. The model produced only small changes in relative humidity throughout the troposphere and thereby provided the first support from such a model for the use of the fixed–relative humidity assumption in estimates of the strength of water vapor feedback. The model's temperature sensitivity was increased over that obtained in the simpler radiative-convective models primarily because of the positive surface albedo feedback, the retreat of highly reflective snow and ice cover near the poles, which amplifies the warming. (This extra warming is not confined to high latitudes, as midlatitude cyclones diffuse some of this extra warming to the tropics as well). The flavor of more recent research on climate sensitivity with global models can be appreciated by sampling some of the efforts listed in the references (34–39).

As climate models have evolved to include realistic geography, predicted cloud cover, and interactions with sea ice and ocean circulation, certain robust conclusions have emerged. In particular, all comprehensive climate models of which we are aware produce increases in water vapor concentrations that are comparable to those predicted by fixing the relative humidity. Differences in equilibrium sensitivity among different models appear to be due primarily to differences in cloud prediction schemes and, to some extent, the treatment of sea ice, and only in a minor way to differing predictions of water vapor distribution. This point was made very clearly by the intercomparison study of Cess et al (40), in which a variety of atmospheric models in an idealized setting were subjected to a uniform increase in surface temperature. The changes in net radiation at the top of the atmosphere in the clear sky were generally consistent across the different models, and consistent with fixed relative humidity radiative computations. The total-sky (clear plus cloudy) fluxes were much less consistent across models.

Recently, Hall & Manabe (41) have artificially removed the radiative consequences of increasing water vapor from a full coupled atmosphere-ocean climate model. The sensitivity of their model is reduced by more than a factor of 3.5. As described in the following section, this large response can be understood, to a rough first approximation, by taking into account how water vapor feedback can interact with other feedbacks.

The Simplest Feedback Analysis

We can take ice/snow albedo feedback into account schematically by assuming that I in equation 1 is a function of T . We then have instead of equation 7,

$$\frac{dT}{d\log_2 CO_2} = \frac{\Delta_0}{1 - \beta_{H_2O} - \beta_I}, \quad 9.$$

where

$$\beta_I \equiv \frac{\partial S}{\partial I} \frac{\partial I}{\partial T} / \frac{\partial R}{\partial T}. \quad 10.$$

Suppose that the strength of the ice/snow albedo feedback has the value of $\beta_I = 0.2$. In the absence of water vapor feedback, albedo feedback of this strength increases the temperature response to CO_2 doubling from 1 K to ≈ 1.25 K. However, in the presence of water vapor feedback of strength $\beta_{H_2O} = 0.4$, albedo feedback increases sensitivity from 1.67 K to 2.5 K. The key here is that the water vapor and ice/snow albedo perturbations feed on each other, with less ice implying warmer temperatures, implying more water vapor, and so on. The existence of strong water vapor feedback increases the importance of other temperature-dependent feedbacks in the system.

Suppose now that we have a variety of models, all with $\beta_{H_2O} \approx 0.4$, but that produce sensitivities from 1.5–4.5 K for doubling of CO_2 , owing to differing treatments of other temperature-dependent feedbacks (cloud cover as well as ice and snow). Figure 4 shows the range of sensitivities that would result if β_{H_2O}

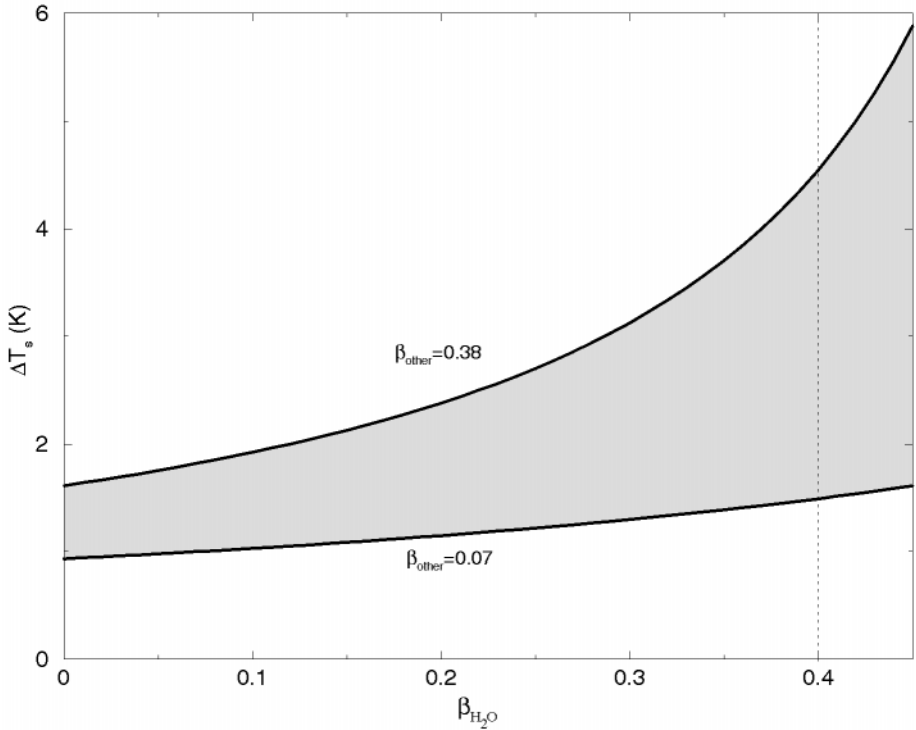


Figure 4 The change in surface temperature ΔT_s for doubled CO_2 as a function of the water vapor feedback parameter $\beta_{\text{H}_2\text{O}}$. Results are shown for two different scenarios of other temperature-dependent feedbacks β_{other} that encompass the current range of predictions in $\Delta T_s = 1.5\text{--}4.5\text{ K}$ when $\beta_{\text{H}_2\text{O}} = 0.4$.

had a smaller value in these models. If there were no water vapor feedback, the maximum sensitivity would be close to 1.5 K, which is the minimum sensitivity for $\beta_{\text{H}_2\text{O}} = 0.4$. The figure also predicts a result roughly consistent with the Hall and Manabe coupled model in which water vapor feedback alone is suppressed, given that that model's sensitivity is greater than 3.5 K for CO_2 doubling.

Because cloud and water vapor feedbacks are obviously related at some level, they are often confused in popular discussions of global warming. In the current generation of climate models, water vapor feedback is robust and cloud feedback is not. A robust water vapor feedback sensitizes the system, making the implications of the uncertainty in cloud feedbacks of greater consequence.

The total radiative effect of increases in water vapor can be quite dramatic, depending on the strengths of the other feedbacks in the system. For the remainder of this review we return our focus to water vapor feedback in isolation, represented by $\beta_{\text{H}_2\text{O}}$ in the preceding discussion.

THE CLIMATOLOGICAL RELATIVE HUMIDITY DISTRIBUTION

The Global Picture

In Arrhenius' and Chamberlin's time, discussions of water vapor feedback necessarily took place without knowledge of the climatological distribution of humidity except near the Earth's surface. With the advent and continued maintenance of the remarkable network of twice-daily balloon ascents, designed for weather forecasting after World War II, the climatological water vapor distribution throughout the troposphere began to be defined with greater clarity. However, the routine measurement of water vapor, especially in the upper troposphere, is inherently more difficult than that of temperature and winds, owing in part to problems of contamination as instruments pass through the far wetter lower troposphere. [See Elliott & Gaffen (42) on the difficulties in using the water vapor fields from the weather balloon, or radiosonde, network for climate studies.] Additionally, there are relatively few radiosonde ascents in the dry subtropical regions of special interest to the water vapor feedback debate.

Satellites fill this gap nicely, however. By measuring the upwelling radiance in different spectral bands that are sensitive to absorption by water vapor, one can obtain measurements of water vapor concentrations in various parts of the atmosphere (43). An example of our current remote sensing capabilities is shown in Figure 5 (see color insert), which depicts the distribution of relative humidity averaged over the upper troposphere. Note the presence of deep convective clouds (*white*), detraining cirrus anvils (*gray*), the convective moistening of adjacent regions of high relative humidity (*red*), and the gradual reduction in relative humidity as air is expelled from convective towers and is carried towards the subtropics, subsiding and warming owing to adiabatic compression along the way, ultimately resulting in relative humidities <10%. An international network of satellites provides global observations of water vapor several times a day and has greatly enhanced our understanding of its distribution and its radiative effects. Although the measurements shown in Figure 5 are limited to cloud-free regions, satellite sensors capable of penetrating cloud cover also exist, thus enabling observations of water vapor under nearly all weather conditions. Whereas better observations would allow us to test models more definitively, the existing radiosonde/satellite database leaves little room for major surprises concerning the climatological distribution of water vapor in the troposphere.

Operational weather prediction centers gather water vapor, temperature, and wind data from all available sensors, including satellites and radiosondes, and combine these with predictions from previous forecasts to generate their best estimate of the current atmospheric state for use as the initial condition for the next forecast. Figures 6 and 7 show the relative humidity fields generated by the European Centre for Medium-Range Weather Forecasting, averaged in time over the month of July 1987. Figure 6 is an average over longitude. Figure 7 is a horizontal map of the vertical average over the free troposphere, excluding the

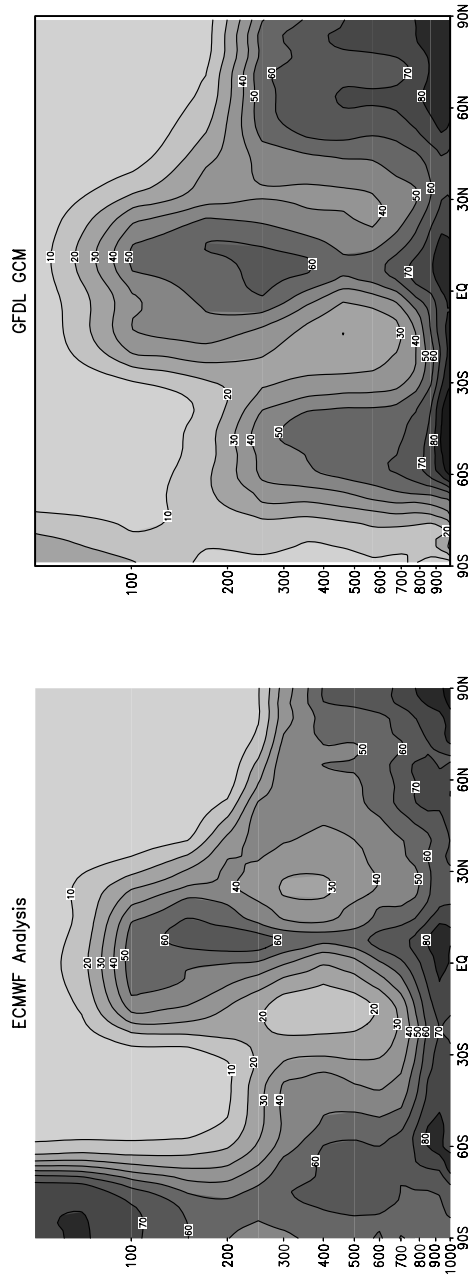


Figure 6 Height-latitude cross sections of the zonal-mean relative humidity for July 1987 as produced by the European Centre for Medium-Range Weather Forecasts (ECMWF) analysis system (*left*) and predicted by the GFDL (Geophysical Fluid Dynamics Laboratory) General Circulation Model (GCM) (*right*).

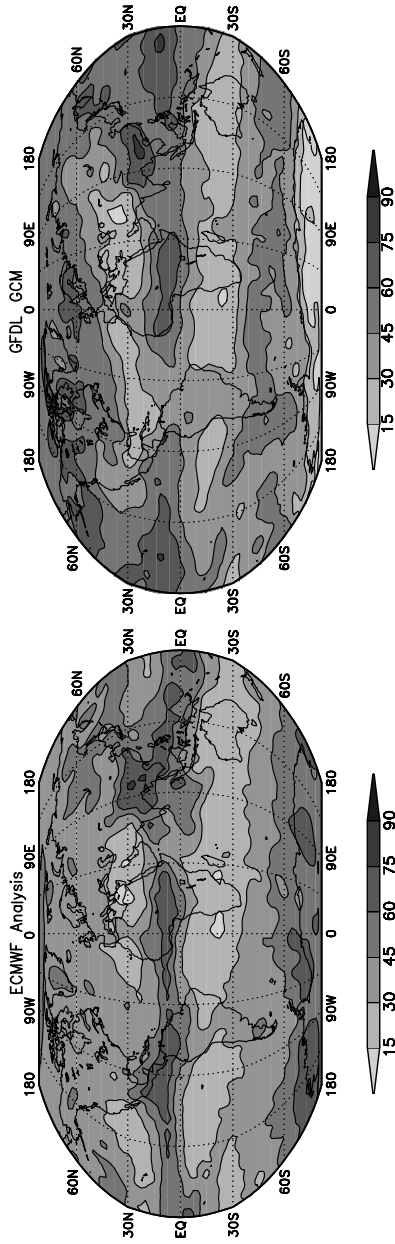


Figure 7 The geographic distribution of relative humidity, vertically averaged over the free troposphere for July 1987 from the ECMWF (European Centre for Medium-Range Weather Forecasts) analyses (*left*) and the GFDL GCM (Geophysical Fluid Dynamics Laboratory General Circulation Model) (*right*).

lowest 2 km. Also shown are the comparable relative humidities from a climate model in use for global warming and atmospheric dynamics studies in our laboratory (34, 44), assuming as a surface boundary condition the observed sea surface temperatures from the same time period.

The general features of the humidity distribution are similar in both the operational analyses and the General Circulation Model (GCM). Note the high values of relative humidity within the planetary boundary layer near the surface; the intermediate values in the free troposphere in midlatitudes, the dryness of the subtropics, and the high values near the equatorial tropopause. Detailed evaluations of the GCM climatologies indicate that most models compare favorably with satellite observations of the vertically-integrated water vapor mass, although there is a tendency in many GCMs to underestimate the water vapor concentrations by about 5% (45, 46).

The Planetary Boundary Layer

In the planetary boundary layer, the lowest 1–2 km, strong vertical turbulent mixing strives to create a layer of uniform mixing ratio, which given the decrease in temperature with height forces the relative humidity to increase with height. This mixing results in a layer of maximum cloudiness near the top of this layer, and dries the air in the immediate vicinity of the surface, reducing the relative humidity in the lower parts of the boundary layer to $\approx 80\%$, on average.

Most of the Earth’s surface is ocean, and evaporation E from the ocean can be modeled as proportional to the difference between the saturation vapor pressure at the surface temperature T_* and the vapor pressure in the atmosphere at some small convenient reference height (typically taken to be 10 m), where the temperature is T_a and the relative humidity is H_a :

$$E \approx C[e_s(T_*) - H_a e_s(T_a)]. \tag{11}$$

The constant of proportionality C is itself roughly proportional to the wind speeds at this reference height. We can rewrite this expression as

$$E \approx C[e_s(T_*)(1 - H_a) + H_a(e_s(T_*) - e_s(T_a))]. \tag{12}$$

The temperature difference $T_* - T_a$ is small enough (especially in the tropics, where E is the largest) that the term proportional to $1 - H_a$ is the larger of the two terms in Equation 12. Suppose the surface and atmosphere both warm by 2 K and the vapor pressure in the atmosphere does not increase. H_a would decrease from ≈ 0.8 to ≈ 0.7 , and $1 - H_a$ would increase by $\approx 50\%$. The surface winds are highly unlikely to change dramatically enough to compensate for this large effect. The energy for this increased evaporation would have to come from the net downward radiation at the surface, which cannot plausibly change by this amount for such a small temperature change. On this aspect of the problem there is little controversy: Water vapor in the boundary layer will increase as climate warms to prevent the near-surface relative humidity from decreasing appreciably.

The Free Troposphere

It is useful to have in mind an explicit, even if oversimplified, picture of the maintenance of subsaturation in the free troposphere in order to appreciate the patterns in Figures 6 and 7 and discuss their sensitivity. Recall first that the water vapor mixing ratio r is conserved as air parcels are carried by the winds, except for the sources and sinks of vapor. Assume that an air parcel is brought to saturation whenever it comes within the planetary boundary layer, and that this is the only source of vapor. Assume also that whenever e rises above e_s , condensation immediately reduces e to e_s and that rain removes all condensate instantaneously without moistening the underlying atmosphere.

Now pick a location within the atmosphere, \mathbf{x} , with temperature T and pressure p . The mixing ratio at this point, at a particular time, can be computed by examining the trajectory of the air parcel at this location. Assuming that the parcel is not saturated, follow this trajectory backwards in time until one encounters the point at which saturation last occurred. Label the temperature and pressure at this point T_c and p_c . (If the parcel is already saturated, set $T_c = T$ and $p_c = p$.) In general, this condensation point will occur at lower pressure $p_c < p$, where T_c is sufficiently cold; an unsaturated parcel has most likely subsided since it was last saturated. The vapor pressure at this point is $e_s(T_c)$. Conserving mixing ratio along the trajectory, one finds that vapor pressure at the original point \mathbf{x} is given by $(p/p_c)e_s(T_c)$. To compute the time-averaged vapor pressure, one needs to think of T_c and p_c as suitably averaged using the ensemble of trajectories that pass through \mathbf{x} at different times. As climate changes, the degree of subsaturation at \mathbf{x} will be affected by changes in $T(\mathbf{x})$ and in T_c and p_c . In practice the changes in p_c are not very important, and we can think of $e \propto e_s(T_c)$. It is not difficult to show that fixing $T - T_c$ is now practically equivalent to fixing H . Therefore, within this simple model, the assumption of fixed relative humidity is in practice equivalent to the assumption that the change in the temperature of last saturation is on average similar to the temperature change itself.

The most important effects ignored in this picture are those due to transport and subsequent re-evaporation of the condensed phase. We return to this complication below.

One can imagine the change in T_c differing from the change in T for a variety of reasons. For example, one can imagine that the warming is spatially uniform but that the vertical excursions of air parcels increase in extent, so that the typical parcel reaching point \mathbf{x} last experienced saturation at a higher altitude where the temperature is colder, thereby causing T_c to increase less than it otherwise would. The result would be an increase in $T - T_c$ and a reduction in H . The assumption of fixed $T - T_c$ or H can be thought of as a conservative stance in the absence of convincing demonstrations to the contrary from models of the atmospheric circulation.

Outside of the tropics, poleward of $\approx 30^\circ$, the cyclones and anticyclones exert primary control on the relative humidity above the boundary layer (47). In these extratropical circulations, typical trajectories projected onto the latitude-vertical

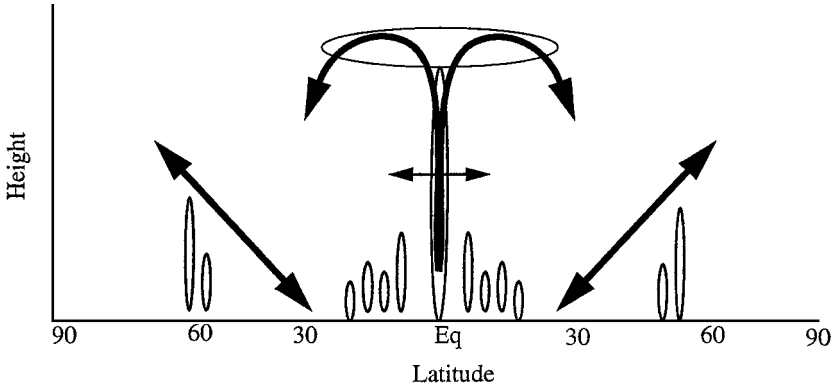


Figure 8 A height-latitude schematic of the large-scale atmospheric trajectories involved in the transport and mixing of moisture within the troposphere.

plane are as shown schematically in Figure 8, with poleward moving air rising and equatorward moving air descending. The slopes of these trajectories typically take air from the boundary layer in the subtropics to the tropopause in subpolar latitudes. Relatively dry air is produced by lifting moist subtropical boundary layer air along these slantwise paths in the warm sectors of extratropical waves, precipitating out much of this water, and then descending while returning equatorward.

With this picture in mind, there is no reason to expect that relative humidity will be exactly maintained in this region as the climate warms. Changes in the strength or paths of the mid-latitude storms, and the associated trajectories of air parcels, could alter the relation between the local temperature change and the average temperature change at the point of last saturation. However, the scale of these storms is relatively large and reasonably well simulated in climate models. Changes in the extratropical circulation predicted by these models, although potentially of consequence for regional weather patterns, are not large enough to substantially modify the relative humidity of the extratropical atmosphere as a whole. Distortions due to subgrid scale processes are less worrisome in extratropical latitudes than in the tropics, and there is less reason to question the generic model prediction of small changes in relative humidity.

Before turning to the tropics, we pause to explain why the free troposphere in the tropics is of primary concern in any analysis of water vapor feedback.

RELATIVE IMPORTANCE OF DIFFERENT PARTS OF THE TROPOSPHERE FOR WATER VAPOR FEEDBACK

Fix attention on a horizontal location at a particular time of year. Given the vertical profile of temperature, water vapor, and cloud aerosols, and the CO_2 concentration, we can compute the outgoing infrared flux R using a radiative model. Fixing clouds

and CO₂, and dividing up the atmosphere in the vertical into a number of layers N , we can think of R as a function of the surface temperature and of the temperature and the water vapor pressure in each of these layers. We can then linearize around the values of these temperatures and water vapor pressures in the current climate to compute the sensitivity of R to each of these values

$$\delta R = \sum_{k=1}^N \left[\frac{\partial R}{\partial T_k} \delta T_k + \frac{\partial R}{\partial e_k} \delta e_k \right]. \tag{13}$$

Rather than treat the dependence on surface temperature separately, we assume that the change in temperature at the surface is equal to the change in temperature in the lowest atmospheric layer, and include the response to the surface temperature change in $\partial R/\partial T_k$ within the lowest layer.

The vapor pressure change required to maintain fixed relative humidity, H , in the face of a small temperature change δT is $H(de_s/dT)\delta T$. If (a) H is assumed to be unchanged and if (b) the temperature change is spatially uniform, then

$$\delta R = \sum_{k=1}^N [Q_T^k + Q_e^k] \delta T, \tag{14}$$

where

$$Q_T^k \equiv \frac{\partial R}{\partial T_k}; \quad Q_e^k \equiv \frac{\partial R}{\partial e_k} H \frac{de_s}{dT}. \tag{15}$$

The temperature change that produces a given global and annual mean change in outgoing infrared radiation δR is

$$\delta T = \frac{\delta R}{M_T + M_e} = \frac{\delta R/M_T}{1 - \beta_{H_2O}}, \tag{16}$$

where

$$M_T \equiv \overline{\sum_{k=1}^N Q_T^k}; \quad M_e \equiv \overline{\sum_{k=1}^N Q_e^k} \tag{17}$$

and

$$\beta_{H_2O} = -\frac{M_e}{M_T}. \tag{18}$$

The overbar refers to an average over latitude, longitude, and season.

Figure 9 (see color insert) shows a particular estimate of the functions Q_e and Q_T obtained by the authors. We divide the atmosphere into 10 layers of equal mass in the vertical, use temperature and humidity data from the European Centre for Medium-Range Weather Forecasting, and cloud data from the International Satellite Cloud Climatology Project (48). We also average over longitude for display purposes, and show the result for July only. We obtain from these results that

$\beta_{H_2O} \approx 0.33$ owing to infrared effects alone. Solar absorption, not discussed in detail here, increases this to ≈ 0.38

The function Q_T is strongly affected by the cloud distribution. Where upper level clouds are prevalent, the outgoing infrared radiation is most sensitive to temperatures at the level of these emitting surfaces, and is relatively insensitive to temperatures deeper in the atmosphere. Where skies are clearer, lower tropospheric temperatures control the outgoing flux.

The function Q_e provides one view of the relative importance of different levels and latitude zones for the strength of the infrared water vapor feedback. If temperatures change uniformly and if relative humidities remain unchanged, this figure tells us how much of the reduction in outgoing radiation is due to the water vapor in different regions. One sees that the middle and upper troposphere dominates the feedback under these conditions. This is a critical and at first glance, perhaps, a surprising result, given the distribution of vapor, which thins very rapidly as one moves upwards. The centers of water vapor spectral lines are fully saturated under atmospheric conditions, and the photons emitted from the lower troposphere can only escape to space if they are emitted from the wings of spectral lines, where the upper tropospheric absorption is sufficiently weak but where the emission is correspondingly inefficient. Emission from the upper troposphere occurs closer to the centers of these lines, where the emission is stronger.

Figure 9 shows that the subtropical dry zones are somewhat more important than the moister zone in the deep tropics for the strength of the fixed relative humidity water vapor feedback. This feature is a consequence of the presence of clouds. If clear skies are assumed to exist everywhere, the maximum in this figure shifts to the moister regions in the tropics.

The question of the relative importance of different regions for water vapor feedback is a source of some confusion in the literature. In assessing this relative importance, one approach has been to assume equal fractional perturbations in mixing ratio (or, equivalently, vapor pressure), as in Shine & Sinha (6):

$$\delta e \propto e. \tag{19}$$

Alternatively, Spencer & Braswell (49) perturb the relative humidities in different regions by equal amounts, so that

$$\delta e \propto e_s, \tag{20}$$

which weights dry regions more strongly, thereby emphasizing the free troposphere at the expense of the boundary layer and the subtropics over the tropics, as compared with Shine & Sinha. With the normalization we have chosen, the upper troposphere is also weighted more heavily than in Shine & Sinha because the assumption of fixed relative humidity for a uniform temperature change requires

$$\delta e \propto \frac{e}{e_s} \frac{de_s}{dT} \propto \frac{e}{T^2}. \tag{21}$$

However, the weight of the subtropics versus the tropics, which have similar temperatures, is similar to that obtained with Equation 19; the dry subtropics are weighted much less heavily than in Spencer & Braswell (49).

There is no ambiguity as to how to compute the relative importance of different regions for water vapor feedback in a model that predicts changes in water vapor concentrations; the confusion only arises from differing presumptions as to a plausible model-independent starting point. Our justification for Equation 21 is only that it better resembles GCM predictions.

Low resolution can make a climate model too diffusive and can result in the dry regions of the troposphere being too moist. Yet the radiative transfer is such that, for a given temperature profile, changes in the absorptivity are roughly proportional to changes in the logarithm of the water vapor concentration (24). If the changes in vapor pressure are proportional to the vapor pressure itself (as in Equations 19 or 21) the impact on sensitivity of such errors in mean humidity is small. Only if one assumes that the fractional changes in vapor pressure are much larger in dry than in moist regions, as implied by Equation 20, can one argue that the absence of very dry regions in a climate model seriously distorts the sensitivity.

An additional source of confusion is that some studies assume clear skies in the radiative computation. This has the consequence of inappropriately weighting the lower troposphere, since clouds interfere with the outgoing infrared radiation emitted by the lower troposphere more frequently than that from the upper troposphere. If we regenerate Figure 9 (*top*) assuming clear skies, the maximum values occur much lower in the troposphere, in the 500–600 millibar (mb) layer.

If temperature changes are uniform and relative humidities remain unchanged as the climate warms, these results show that the humidity response in the free troposphere above 800 mb is responsible for almost all of the infrared water vapor feedback, leaving only 10% to be contributed by the boundary layer. Roughly 55% of the total is due to the tropical free troposphere (30N–30S) (N = North; S = South), and 35% to the extratropics. Of this tropical contribution, about two-thirds, 35% of the total, is due to the upper half of the troposphere, from 100–500 mb.

If relative humidity does change and if the temperature changes are not spatially uniform, one can generalize Equation 16 to read

$$\delta T_* = \frac{\delta R}{M_T + M_e} = \frac{\delta R/M_T}{1 - \beta_{H_2O}}, \quad 22.$$

where now

$$M_T \equiv \overline{\sum_{k=1}^N Q_T^k \delta \tilde{T}_k}; \quad M_e \equiv \overline{\sum_{k=1}^N Q_e^k \delta \tilde{e}_k \delta \tilde{T}_k}. \quad 23.$$

δT_* is the change in mean surface temperature, $\delta \tilde{T}$ is the temperature change normalized by δT_* , and $\delta \tilde{e}$ is the vapor pressure change normalized by the vapor pressure change required to maintain fixed H . The kernels Q_T^k and Q_e^k in Figure 9 are unchanged.

The temperature changes predicted by climate models are not spatially uniform. A very robust feature across models is the polar amplification of the temperature signal, which implies that $\delta\tilde{T}$ is larger than unity in high latitudes, thereby enhancing the extratropical as opposed to the tropical contribution to water vapor feedback. Of potentially greater importance, many climate models predict that warming in the tropics will be larger in the upper troposphere than in the lower troposphere (50), ultimately because the moist adiabatic lapse rate decreases with increasing temperature. If this is the case, and if H is fixed, the tropical upper troposphere becomes even more dominant in its contribution to M_e . But M_T also increases in value, because the outgoing infrared radiation is sensitive to the temperature of the cloud tops [as in Figure 9 (*bottom*)]. As a result, the value of β_{H_2O} does not increase significantly. In fact, we have found it difficult to raise β_{H_2O} much above 0.4 for any plausible temperature change profiles, with fixed relative humidity. [We caution the reader that water vapor feedback is often defined with $\delta\tilde{T} \equiv 1$ in M_T (21, 51)]. Similarly, estimates of β_{H_2O} are also insensitive to modest biases in the water vapor climatology that may be present in a climate model. For example, introducing a dry bias of 5%, which is typical of that found in many GCMs (45, 46), into the humidity climatology used in Figure 9 results in less than a 3% bias in the corresponding estimate of β_{H_2O} .

Extending the approach of Hall & Manabe (41), one can artificially remove the effect of the water vapor perturbations on radiative fluxes in a climate model, but only in one region at a time. Schneider et al (52) have recently presented an analysis of this kind, which suggests that extratropical moisture is of greater importance for climatic sensitivity than is implied by the purely radiative computations leading to Figure 7. The reasons for this difference are unclear at present.

THE CONTROVERSY CONCERNING WATER IN THE TROPICAL FREE TROPOSPHERE

The Complexity of the Tropics

When different groups attempt to construct numerical simulations of an incompletely understood complex system, one might hope that intercomparisons of the sort described by Cess et al (40) would indicate where the major uncertainties lie. But it is also possible that all models are making similar mistakes. Indeed, it has been argued that global climate models all err in their treatment of water vapor in similar ways, particularly in the tropics (53–57). The source of this concern is the fact that much of the vertical transport of heat, momentum, and moisture in the tropics occurs on scales of a few kilometers or less, in turbulent eddies generated by moist convection, scales that are not explicitly resolved in global climate models.

Figure 10 (see color insert) is a scene from a numerical simulation (58) of a small part of the tropical atmosphere, with horizontal extent $130 \text{ km} \times 130 \text{ km}$,

which is about the the size of a single grid cell in a global climate model. This simulation has a horizontal resolution of 2 km, which is barely sufficient to resolve the energy-containing eddies of the moist convective turbulence that dominates the convectively active parts of the tropics. Such models have been under development for several decades, but it is only recently that computer power has become sufficient that they can be integrated over the time required for the atmosphere to equilibrate, through radiative and convective fluxes, with the underlying surface, even over such small domains (59–62). We estimate that a research group would require at least a petaflop (10^{15} floating point operations per second) of computer power to perform useful climate sensitivity experiments with a global model at this resolution. Unfortunately, we already know that models of this class are themselves dependent in important ways on assumptions concerning cloud microphysics, the micron-scale physics of individual water drops that controls the cloud droplet (and ice particle) size distributions to which the radiative transfer, among other things, is sensitive.

It is the existence of these layers of complexity on ever smaller scales, which potentially play a particularly important role in the tropics, that fuels the debate on the reliability of GCM climate predictions and the robustness of water vapor feedback in particular.

One can sense an increasing uneasiness, and an increasing focus on the tropical upper troposphere, in this series of excerpts from the reports of the Intergovernmental Panel on Climate Change from 1990, 1992, and 1995.

1990: “The best understood feedback mechanism is water vapor feedback, and this is intuitively easy to understand” (63).

1992: “There is no compelling evidence that water vapor feedback is anything other than positive—although there may be difficulties with upper tropospheric water vapor” (64).

1995: “Feedback from the redistribution of water vapor remains a substantial source of uncertainty in climate models—Much of the current debate has been addressing feedback from the tropical upper troposphere” (65).

At least three distinct mechanisms have been suggested by which changes in moist convection in the tropics could reduce the strength of water vapor feedback. As the climate warms, the temperature of the upper tropospheric outflow from the convective cores could increase less than the temperature itself; the condensate amounts in this upper tropospheric outflow could decrease; and the precipitation efficiency of the convection could increase.

Convective Outflow Temperatures

A simple picture that serves as a starting point for thinking about the tropical circulation is one in which air is subsiding everywhere except in convectively active areas in which there is concentrated upward motion. The subsidence is weak, requiring a few weeks to take air from the upper troposphere to the boundary

layer; its strength is determined by the rate at which the air cools radiatively. The upward motion is much stronger, and is confined to a small fraction of the total area. The outflow from these convective areas is at its largest near 200 mb, just below the tropopause. When air emerges in this outflow it is at or near saturation, as in Figure 5. As the air subsides, the adiabatic warming due to compression accompanying the descent will produce relative humidities as low as a few percent before reaching the boundary layer, assuming that no moisture is added to the parcel.

In this simple picture of the tropics, the relative humidity is tightly coupled to the characteristic temperature of these convective outflows beneath the tropopause, as this will be the temperature of last saturation, T_c , for much of the tropical troposphere. R Lindzen's initial critique of water vapor feedback (53) argued that this outflow temperature should, in fact, warm less than the temperature at a fixed location in the troposphere; it might possibly even cool as the troposphere warms. One expects deeper convection in a warmer atmosphere, in which the boundary layer air contains more moisture. If the height of the convection increases enough that the extra cooling obtained by following a moist adiabatic profile to higher levels over-compensates the warming at a given level, T_c would decrease and water vapor feedback from the bulk of the tropical troposphere would be negative. Even if T_c increases, but not as much as T itself, the positive water vapor feedback would still be weakened.

The depth of moist convection does increase in all climate models as the climate warms. The characteristic temperature of the outflow from the deepest convective cells must therefore increase less than does the temperature at fixed height. One might expect these models to show large reductions in tropical relative humidity on this basis, but this does not occur. It has sometimes been argued that numerical deficiencies prevent the memory of the water vapor mixing ratio from being retained during the slow descent through the model's troposphere. However, in a recent study it has been shown that air parcel trajectories accurately computed from the wind fields generated by a global model predict humidity distributions that differ only slightly from the distribution in the model (66). A far more plausible explanation is that air parcel trajectories in the tropics are more complex than envisioned in this simple picture.

The tropical atmosphere is far moister than it would be if most of the air in the tropics last experienced saturation just below the tropopause. Yet detailed studies of observed air parcel trajectories (67–69) confirm that the tropical humidity distribution in the free troposphere can indeed be understood by following trajectories backwards in time to obtain the temperature of last saturation. Several elements must be added to our idealized picture of the tropics to make it more realistic. When moist convection occurs, a spectrum of convective cores of different vertical extents expel saturated parcels at different levels, and horizontal motions carry air into and away from convective centers throughout the troposphere, mixing moisture into drier regions. Finally, whereas some of air in the very driest parts of the tropics can be traced back directly to the cold trap at the top of the deepest convective cores, some of this air is also mixed in from mid-latitudes (70).

More research is required to understand how the statistics of this complex set of trajectories changes as climate warms, so as to better understand why the relative humidities in models do not decrease as much as one might suspect based on the change in temperature of the deepest convective outflows.

Condensate

Cloud anvils form near the tops of convective regions, and the more condensate (primarily ice) that is held in these regions without precipitating, the moister the atmosphere will be. As an air parcel is expelled from a convective region and begins to subside and warm, this ice must first sublime or fall and evaporate into unsaturated layers before the relative humidity can begin to fall. One can argue that the relative humidity of the tropics will decrease if the amount of condensate produced in the convective outflows decreases (56).

A prerequisite for the plausibility of this argument is robust evidence for an effect of condensate on the present-day humidity distribution, since we require this effect to weaken as the climate warms in order to weaken the water vapor feedback. This case has not been made convincingly. Indirect evidence to the contrary is provided by the tropical trajectory studies referenced earlier, in which models with no condensate are able to reproduce much of the observed humidity distribution. Additionally, many climate models attempt to incorporate prediction equations for the condensed phases of water. While modifications to these schemes certainly have a dramatic influence on cloud feedback (71), there are no reports that the prediction of condensate reduces water vapor feedback.

The intuition on which this argument is based is that the convection in a warmer climate will be more intense, but occupy a smaller fraction of the horizontal area of the tropics at any one time. There is no direct evidence for this claim at present. Convection-resolving models of the sort pictured in Figure 10 (see color insert), when integrated to a radiative-convective equilibrium, albeit in idealized geometries of small spatial extent, generally do not predict a reduction in upper tropospheric ice cloud concentrations as the temperature is increased; to first order they typically predict that the distribution is simply shifted upwards consistent with the deeper troposphere (59, 62).

If there are reductions in upper level cloud coverage in the tropics as climate warms, these will directly reduce climate sensitivity by removing the infrared trapping due to the clouds themselves. The climate modeling community has admitted and been frustrated for years by its inability to converge on robust estimates of such cloud feedbacks. But this uncertainty should not obscure the fact that climate models do all possess a strong water vapor feedback which, as we have seen, sensitizes the system to possible cloud feedbacks, whether positive or negative.

Precipitation Efficiency

Closure schemes for moist convection in climate models differ in their precipitation efficiency—the ratio of the water rained out to that condensed, the remainder

re-evaporating as it falls and moistening the air. As a result, closure schemes differ in the relative humidity of the mid-troposphere in convecting regions. (Higher in the troposphere, all schemes agree that the atmosphere is quickly driven close to saturation by the convection). It has been argued (55–57) that tropical precipitation efficiency could increase in a warmer world, for microphysical reasons related to an increase in the rate of coalescence of small into large drops, causing the mid-troposphere to dry. The quantitative relevance of this argument is difficult to evaluate in the context of global climate models in which the convective motions are not explicitly resolved.

The issue is more readily addressed in integrations of convection-resolving models in idealized geometries (59, 62). We are unaware of simulations of this type that demonstrate a significant effect of this kind.

This argument is complementary to the previous two, in that it requires that the mid-tropospheric humidity in the convective regions be mixed horizontally into the rest of the tropics. If the bulk of the trajectories pass through the cold trap in the upper troposphere before descending, any information about mid-tropospheric humidities in the convecting regions will be lost. The single-column models of the tropics on which these arguments are typically based provide an extreme limiting case in which the horizontal mixing can be thought of as perfectly efficient, and so overestimate the impact this effect can have on the rest of the tropics, even if one accepts the microphysical arguments.

Empirical Studies

In order to help evaluate these critiques of the treatment of convection in climate models, a variety of studies have been undertaken using satellite data, the radiosonde network, and analyses of the atmospheric state generated through numerical weather prediction. In addition to the trajectory analyses mentioned above, numerous investigators have focused on local relationships between convection and upper tropospheric water vapor (72–76). These studies demonstrate that deep convection serves to moisten the upper troposphere locally and that global climate models are reasonably successful in reproducing the observed relationships between convection and upper tropospheric water vapor on regional scales. Given the need to analyze water spatially integrated over entire circulation systems (77, 78), investigations of such large-scale behavior (27, 28, 79) have also been undertaken, focusing primarily on clear-sky greenhouse trapping rather than humidity itself. The agreement with climate models is often quite impressive, as in Figure 3 and in Inamdar & Ramanathan's study (80) of the sensitivity of the global-mean clear-sky greenhouse trapping to surface temperature.

An exception is the study of Sun & Held (81), in which an attempt is made to use the radiosonde database to relate tropical mean humidity at different levels in the troposphere to the mean surface temperature on El Niño time scales. At face value, the results imply that the humidity increases less rapidly with increasing temperature than in the models examined, and that the observed free tropospheric

humidity and surface temperatures are less strongly coupled than in the model. Sun & Held state that their observed regressions, if applied uncritically to the global warming problem, imply that the model is overestimating the global mean water vapor feedback by $\approx 15\%$. In light of the estimates presented above, we now believe that the stakes are somewhat higher—closer to 25%. However, the adequacy of the radiosonde data for drawing this conclusion is suspect due to the lack of observations over vast regions of the tropical oceans, as Sun & Held themselves observed. Indeed, comparison with satellite observations have clearly highlighted the inability of the radiosonde network to accurately monitor variations in tropical water vapor (82). It is also difficult to reconcile the Sun & Held result with analysis of the tropical mean clear-sky greenhouse trapping (28).

Other pieces of information exist that, taken together, increase our confidence in the existence of strong water vapor feedback. As one example, models with strong water vapor feedback, when forced with ice-age boundary conditions and CO_2 concentrations, produce sea surface temperature changes that are consistent with paleo-data in the tropics (83), although the error bars on ice-age tropical ocean temperatures remain disturbingly large due to the difficulty of reconciling different paleo-temperature indicators.

In addition, the observed twentieth century warming is itself difficult to reconcile with a greatly reduced climate sensitivity. An alternative to the theory that greenhouse gases have been responsible for the bulk of the observed warming is that it is simply due to natural climatic variability. But the natural variability on long time scales is sharply reduced when water vapor feedback is artificially removed from a climate model (41). One can think of stronger “spring constants” as reducing the response to internally generated noise as well as the response to an external force. It is thus doubly difficult to explain the observed twentieth century record with such a stiff model.

Finally, empirical confirmation or refutation of the models will surely emerge eventually from the analysis of trends in water vapor. Some careful regional studies have documented increasing amounts of tropospheric water vapor over North America (84), China (85), and the tropical western Pacific (86). One study of trends over the tropics as a whole (87) claims a downward trend, but the data quality has been questioned (88), and discrepancies are found when compared to other data sets (89). None of these studies focus specifically on upper tropospheric water vapor, for which the radiosonde data are more problematic.

We have examined the tropical water vapor trends simulated in global warming scenarios generated with a model developed in our laboratory. Five realizations have been generated (34) so that one can compare the externally forced signal with the model’s natural variability. The linear trend in the tropical mean water vapor mixing ratio at 200 mb, computed from the years 1965–2000, ranges among the different realizations from a low of 1.5%/decade to a high of 3.7%/decade. The trends near the surface are closer to 1%/decade. This large upper tropospheric moistening is dependent on the fact that the warming in the model tropics is

top-heavy—more so than in the observed warming of the past few decades (50). Therefore, this is an upper bound on the moistening that we expect to be occurring. Even so, the model's natural variability suggests that the current 20-year satellite record is not long enough for unambiguous detection of trends in humidity, even if there were no issues with regard to changing instrumentation.

FINAL REMARKS

No empirical or model/data comparisons suggest that water vapor feedback is negative, even in the tropical upper troposphere. Indeed, models with strong water vapor feedback, comparable to that obtained in simple models with fixed relative humidity, are able to simulate many aspects of the observed structure and variability of the humidity field.

Our tests of models are limited to observations of natural climate variability and thus provide information on the validity of the mechanisms that maintain and modify the distribution of water vapor within the models, rather than direct confirmation of the predictions of increasing vapor accompanying global warming. This difficulty will persist until observed time series are compiled with sufficient accuracy and length to detect trends in water vapor on a global scale. Given the acceleration of the trends predicted by many models, we believe that an additional 10 years may be adequate, and 20 years will very likely be sufficient, for the combined satellite and radiosonde network to convincingly confirm or refute the predictions of increasing vapor in the free troposphere and its effects on global warming.

Current climate models invariably support the estimates of the strength of water vapor feedback obtained from the simplest assumption that relative humidity remains unchanged as climate warms. These numerical models are simply tools we use to generate the climates consistent with our hypotheses regarding the relevant physics, including our hypotheses as to how best to treat unresolved scales of motion. If one has a coherent idea for a mechanism that might reduce climate sensitivity, one should be able to incorporate the idea in an idealized and tentative way into a comprehensive climate model. This would enable the community to quantitatively evaluate competing theories about the strength of water vapor feedback, rather than relying on qualitative arguments. If a weak water vapor feedback climate model could be constructed, climate modelers could then analyze it systematically to see if its fit to data is comparable to or better than other models. No such model currently exists.

ACKNOWLEDGMENTS

We wish to express our thanks to James Fleming for information on the history of climate research, to Jerry Mahlman, Ron Stouffer, V Ramaswamy, and Tony Broccoli for careful readings of an earlier draft, and to Kerry Emanuel and Ray Pierrehumbert for helpful discussions.

Visit the Annual Reviews home page at www.AnnualReviews.org

LITERATURE CITED

1. Fourier JB. 1827. Memoire sur les temperatures du globe terrestre et des espaces planétaires. *Mem. Acad. R. Sci. Inst. France* 7:569–604
2. Tyndal J. 1861. On the absorption and radiation of heat by gases and vapours, and on the physical connexion of radiation, absorption, and conduction. *Philos. Mag.* 22:169–94, 273–85
3. Fleming JR. 1998. *Historical Perspectives on Climate Change*. New York: Oxford Univ. Press 194 pp.
4. Clough SA, Kniezys FX, Davies RW. 1992. Line shape and the water vapor continuum. *Atmos. Res.* 23:229–41
5. Tipping R, Ma Q. 1995. Theory of the water vapor continuum and validations. *Atmos. Res.* 36:69–94
6. Shine KP, Sinha A. 1991. Sensitivity of the earth's climate to height-dependent changes in the water vapour mixing ratio. *Nature* 354:38–84
7. Fels SB, Keihl JT, Lacis AA, Schwarzkopf MD. 1991. Infrared cooling rate calculations in operational general circulation models: comparison with benchmark computations. *J. Geophys. Res.* 96(D5):9105–20
8. Ellingson RG, Ellis J, Fels S. 1991. The intercomparison of radiation codes used in climate models: longwave results. *J. Geophys. Res.* 96:8929–53
9. Cess RC, Zhang MH, Minnis P, Corsetti L, Dutton EG, et al. 1995. Absorption of solar radiation by clouds: observations versus models. *Science* 267:496–99
10. Arrhenius S. 1896. On the influence of carbonic acid in the air upon the temperature of the ground. *Philos. Mag.* 41:237–76
11. Chamberlin TC. 1899. An attempt to frame a working hypothesis of the cause of glacial periods on an atmospheric basis. *J. Geo.* 7:609–21
12. Callendar GS. 1938. The artificial production of CO₂ and its influence on temperature. *Q. J. R. Meteorol. Soc.* 64:223–37
13. Plass GN. 1956. The CO₂ theory of climatic change. *Tellus* 8:140–53
14. Kaplan LD. 1960. The influence of CO₂ variations on the atmosphere heat balance. *Tellus* 12:204–8
15. Moller F. 1963. On the influence of changes in CO₂ concentration in air on the radiation balance of Earth's surface and on climate. *J. Geophys. Res.* 68:3877–86
16. Sagan C. 1962. Structure of the lower atmosphere of Venus. *Icarus* 1:151–69
17. Manabe S, Strickler RF. 1964. On the thermal equilibrium of the atmosphere with a convective adjustment. *J. Atmos. Sci.* 21:361–85
18. Manabe S, Wetherald RT. 1967. Thermal equilibrium of the atmosphere with a given distribution of relative humidity. *J. Atmos. Sci.* 24:241–59
19. Ramanathan V, Coakley JA Jr. 1979. Climate modeling through radiative-convective models. *Rev. Geophys. Space Phys.* 16:465–89
20. Wetherald RT, Manabe S. 1988. Cloud feedback processes in a general circulation model. *J. Atmos. Sci.* 45:1397–415
21. Zhang MH, Hack JJ, Keihl JT, Cess RD. 1994. Diagnostic study of climate feedback processes in atmospheric general circulation models. *J. Geophys. Res.* 99(D3):5525–37
22. Kasting JF. 1989. Runaway and moist greenhouse atmospheres and the evolution of Earth and Venus. *Icarus* 74:472–94
23. Barkstrom BR. 1984. The earth radiation budget experiment (ERBE). *Bull. Am. Meteorol. Soc.* 65:1170–85
24. Raval A, Ramanathan V. 1989. Observational determination of the greenhouse effect. *Nature* 342:758–62

25. Stephens GL, Greenwald TJ. 1991. Observations of the earth's radiation budget in relation to atmospheric hydrology: I. Clear sky greenhouse effect and water vapor feedback. *J. Geophys. Res.* 96:15311–24
26. Bony S, Duvel JP, Le Treut H. 1995. Observed dependence of the water vapour and clear-sky greenhouse effect on sea surface temperature: comparison with climate warming experiments. *Clim. Dyn.* 11:307–20
27. Allan RP, Shine KP, Slingo A, Pamnet JA. 1999. The dependence of clear-sky outgoing longwave radiation on surface temperature and relative humidity. *Q. J. R. Meteor. Soc.* 125:2103–26
28. Soden BJ. 1997. Variations in the tropical greenhouse effect during El Niño. *J. Clim.* 10:1050–55
29. Bates JJ, Jackson DL, Breon FM, Bergen ZD. 2000. Variability of upper tropospheric humidity 1979–1998. *J. Geophys. Res.* Submitted
30. Bjerknes V. 1904. Das problem vod der wettvorhersage, betrachtet vom standpunkt der mechanik und der physik. *Meteor. Z.* 21:1–7. (Reprinted in English in *The Life Cycles of Extratropical Cyclones*, ed. M Shapiro, S Gronas, pp. 1–4. Boston: Am. Meteorol. Soc.)
31. Richardson LF. 1922. *Weather Prediction by Numerical Process*. New York/London: Cambridge Univ. Press. Reprinted New York: Dover, 1965. 236 pp
32. Bengtsson L. 1999. From short-range barotropic modelling to extended-range global weather prediction: a 40-year perspective. *Tellus* 51:13–32
33. Manabe S, Wetherald RT. 1975. The effects of doubling the CO₂ concentration on the climate of a general circulation model. *J. Atmos. Sci.* 32:3–15
34. Knutson TR, Delworth TL, Dixon KW, Stouffer RJ. 2000. Model assessment of regional surface temperature trends (1949–97). *J. Geophys. Res.* 104:30981–96
35. Meehl GA, Collins W, Boville B, Keihl JT, Wigley TML, Arlaster JM. 2000. Response of the NCAR Climate System Model to increased CO₂ and the role of physical processes. *J. Clim.* In press
36. Mitchell JFB, Johns TC, Gregory JM, Tett SFB. 1995. Climate response to increasing levels of greenhouse gases and sulphate aerosols. *Nature* 376:501–4
37. Roeckner E, Bengsston L, Feitcher J, Lelieveld J, Rodhe H. 1999. Transient climate change with a coupled atmosphere-ocean GCM including the tropospheric sulphur cycle. *J. Clim.* 12:3004–32
38. Stouffer R, Manabe S. 1999. Response of a coupled ocean-atmosphere model to increasing atmospheric carbon dioxide: sensitivity to rate of increase. *J. Clim.* 12:2224–37
39. Timmerman A, Oberhuber J, Bacher A, Esch M, Latif M, Roeckner E. 1999. Increased El Niño frequency in a climate model forced by future greenhouse warming. *Nature* 398:694–96
40. Cess RD, Potter GL, Blanchet JP, Boer GJ, Delgenio AD, et al. 1990. Intercomparison and interpretation of climate feedback processes in 19 atmospheric general circulation models. *J. Geophys. Res.* A 95:16601–15
41. Hall A, Manabe S. 1999. The role of water vapor feedback in unperturbed climate variability and global warming. *J. Clim.* 12:2327–46
42. Elliott WP, Gaffen DJ. 1991. On the utility of radiosonde humidity archives for climate studies. *Bull. Am. Meteor. Soc.* 72:1507–20
43. Soden BJ, Bretherton FP. 1993. Upper tropospheric relative humidity from the GOES 6.7 micron channel: method and climatology for July 1987. *J. Geophys. Res.* 98:16669–88
44. Lau NC, Nath MJ. 1996. The role of the “atmospheric bridge” in linking tropical Pacific ENSO events to extratropical SST anomalies. *J. Clim.* 9:2036–57

45. Gaffen DJ, Rosen RD, Salstein DA, Boyle JS. 1998. Evaluation of tropospheric water vapor simulations from the Atmospheric Model Intercomparison Project. *J. Clim.* 10:1648–61
46. Bates JJ, Jackson DL. 1997. A comparison of water vapor observations with AMIP I simulations. *J. Geophys. Res.* 102:21837–52
47. Yang H, Pierrehumbert RT. 1994. Production of dry air by isentropic mixing. *J. Atmos. Sci.* 51:3437–54
48. Rossow WB, Schiffer RA. 1991. ISCCP cloud data products. *Bull. Am. Meteorol. Soc.* 72:2–20
49. Spencer RW, Braswell WD. 1997. How dry is the tropical free troposphere? Implications for global warming theory. *Bull. Am. Meteorol. Soc.* 78:1097–106
50. Tett SFB, Mitchell JFB, Parker DE, Allan MR. 1996. Human influence of the atmospheric vertical temperature structure. *Science* 274:1170–73
51. Hansen J, Lacis S, Rind D, Russel G, Stone P. 1984. Climate sensitivity. *Geophys. Monogr.* 29, ed. JE Hansen, T Takahashi, 5:130–63. Washington, DC: Geophys. Union
52. Schneider EK, Kirtman BP, Lindzen RS. 1999. Tropospheric water vapor and climate sensitivity. *J. Atmos. Sci.* 36:1649–58
53. Lindzen RS. 1990. Some coolness concerning global warming. *Bull. Am. Meteorol. Soc.* 71:288–99
54. Lindzen RS. 1994. On the scientific basis for global warming scenarios. *Environ. Pollut.* 83:125–34
55. Sun DZ, Lindzen RS. 1993. Distribution of tropical tropospheric water vapor. *J. Atmos. Sci.* 50:1644–60
56. Renno NO, Emanuel KA, Stone PH. 1994. Radiativeconvective model with an explicit hydrological cycle: 1. Formulation and sensitivity to model parameters. *J. Geophys. Res.* 99:14429–41
57. Emanuel K, Pierrehumbert RT. 1996. Microphysical and dynamical control of tropospheric water vapor. In *Clouds, Chemistry, and Climate, NATO ASI Ser. 35*. Springer-Verlag. 260
58. Pauluis O, Balaji V, Held IM. 2000. Frictional dissipation in a precipitating atmosphere. *J. Atmos. Sci.* 57:989–94.
59. Held IM, Hemler RS, Ramaswamy V. 1993. Radiativeconvective equilibrium with explicit two-dimensional moist convection. *J. Atmos. Sci.* 50:3909–27
60. Donner LJ, Seman CJ, Hemler RS. 1999. Three-dimensional cloud-system modeling of GATE convection. *J. Atmos. Sci.* 56:1885–912
61. Xu KM, Randall DA. 1999. A sensitivity study of radiative-convective equilibrium in the tropics with a convection-resolving model. *J. Atmos. Sci.* 56:3385–99
62. Tompkins AM, Craig GC. 1999. Sensitivity of tropical convection to sea surface temperature in the absence of large-scale flow. *J. Clim.* 12:462–76
63. IPCC. 1990. *Climate Change: The IPCC Scientific Assessment*. Cambridge, UK: Cambridge Univ. Press. 365 pp
64. IPCC. 1992. *The IPCC Supplementary Report*. Cambridge, UK: Cambridge Univ. Press. 200 pp
65. IPCC. 1995. *The Science of Climate Change*. Cambridge, UK: Cambridge Univ. Press. 572 pp
66. Salath EP, Hartmann DL. 2000. Subsidence and upper-tropospheric drying along trajectories in a general circulation model. *J. Clim.* 13:257–63
67. Sherwood SC. 1996. Maintenance of the free-tropospheric tropical water vapor distribution: II. Simulation by large-scale advection. *J. Clim.* 9:2919–34
68. Salathe EP, Hartmann DL. 1997. A trajectory analysis of tropical upper-tropospheric moisture and convection. *J. Clim.* 10:2533–47
69. Dessler AE, Sherwood SC. 2000. Simulations of tropical upper tropospheric humidity. *J. Geophys. Res.* submitted

70. Pierrehumbert RT, Roca R. 1998. Evidence for control of Atlantic subtropical humidity by large-scale advection. *Geophys. Res. Lett.* 25:4537–40
71. Senior CA, Mitchell JFB. 1993. Carbon dioxide and climate: the impact of cloud parameterization. *J. Clim.* 6:393–418
72. Rind D, Chiou EW, Chu W, Larsen J, Oltmans S, et al. 1991. Positive water vapour feedback in climate models confirmed by satellite data. *Nature* 349:500–3
73. Del Genio AD, Kovari W Jr, Yao MS. 1994. Climatic implications of the seasonal variation of upper troposphere water vapor. *Geophys. Res. Lett.* 21:2701–4
74. Stephens GL, Randall DA, Wittmeyer IL, Dazlich DA, Tjemkes S. 1993. The earth's radiation budget and its relation to atmospheric hydrology:3. Comparison of observations over oceans with a GCM. *J. Geophys. Res.* 99:4391–950
75. Inamdar AK, Ramanathan V. 1994. Physics of the greenhouse effect and convection in warm oceans. *J. Clim.* 7:715–31
76. Soden BJ, Fu R. 1995. A satellite analysis of deep convection, upper tropospheric humidity and the greenhouse effect. *J. Clim.* 8:2333–51
77. Lindzen RS, Kirtman B, Kirk-Davidoff D, Schneider EK. 1995. Seasonal surrogate for climate. *J. Clim.* 8:1681–84
78. Lau K-M, Ho C-H, Chou M-D. 1996. Water vapor and cloud feedback over the tropical oceans: Can we use ENSO as a surrogate for climatic change? *Geophys. Res. Lett.* 23:2971–74
79. Yang H, Tung KK. 1998. Water vapor, surface temperature and the greenhouse effect—a statistical analysis of tropical-mean data. *J. Clim.* 11:2686–97
80. Inamdar AK, Ramanathan V. 1998. Tropical and global scale interactions among water vapor, atmospheric greenhouse effect and surface temperature. *J. Geophys. Res.* 103:32177–94
81. Sun DZ, Held IM. 1996. A comparison of modeled and observed relationships between interannual variations of water vapor and temperature. *J. Clim.* 9:665–75
82. Soden BJ, Lanzante JR. 1996. An assessment of satellite and radiosonde climatologies of upper tropospheric water vapor. *J. Clim.* 9:1235–50
83. Broccoli AL. 2000. Tropical cooling at the last glacial maximum: an atmosphere-mixed layer ocean simulation. *J. Clim.* 13:951–976
84. Ross RJ, Elliot WP. 1996. Tropospheric water vapor climatology and trends over North America: 1973–93. *J. Clim.* 9:3561–74
85. Zhai P, Eskridge RE. 1997. Atmospheric water vapor over China. *J. Clim.* 10:2643–52
86. Gutzler DS. 1996. Low-frequency ocean-atmosphere variability across the tropical western Pacific. *J. Atmos. Sci.* 53:2773–85
87. Schroeder SR, McGuirk JP. 1998. Widespread tropical atmospheric drying from 1979–1995. *Geophys. Res. Lett.* 25:1301–4
88. Ross RJ, Gaffen DJ. 1998. Comment on “Widespread tropical atmospheric drying from 1979–1995” by Schroeder and McGuirk. *Geophys. Res. Lett.* 25:4357–58
89. Soden BJ, Schroeder SR. 2000. Decadal variations in tropical water vapor: A comparison of observations and a model simulation. *J. Clim.* 13:3037–40

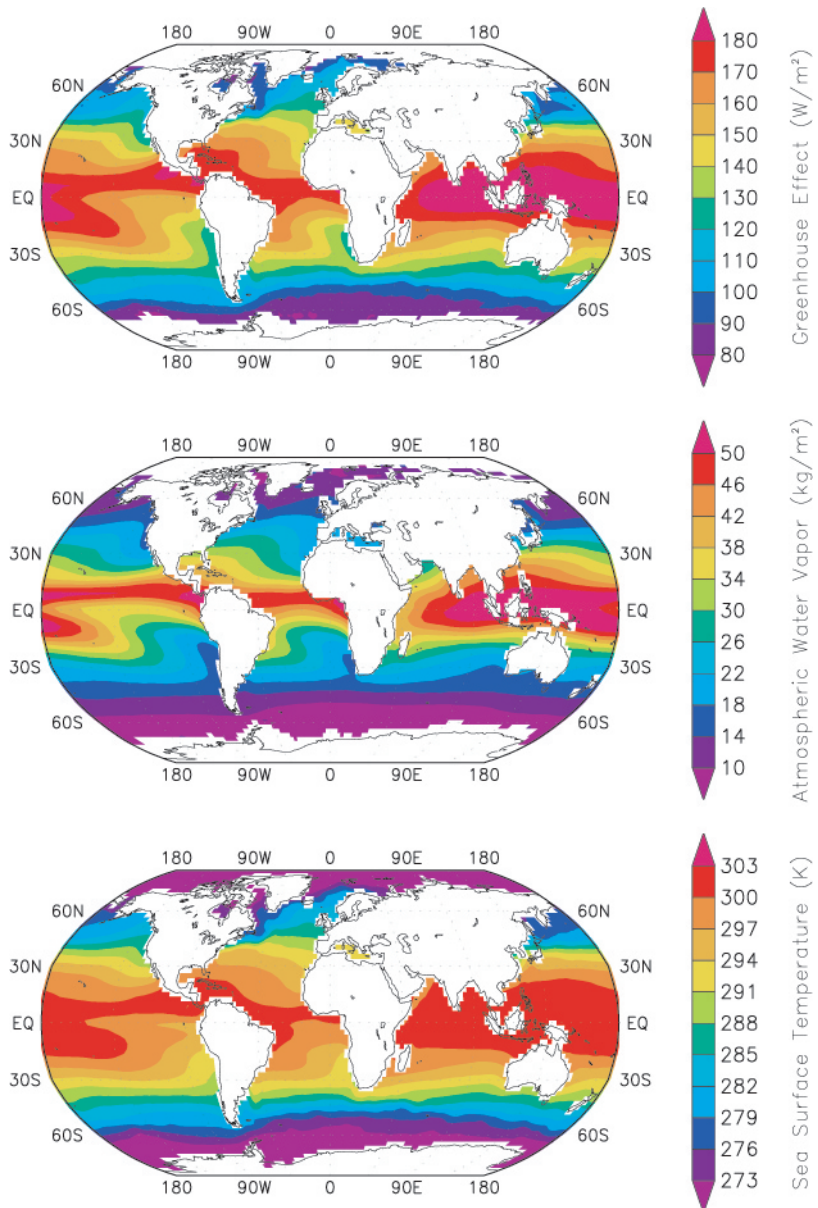


Figure 2 The annual-mean observed distribution of the clear-sky greenhouse effect G_{clear} (top), vertically-integrated water vapor concentration (middle), and sea surface temperature (bottom). Data are missing over land and ice-covered oceans due to uncertainties in their surface emission.

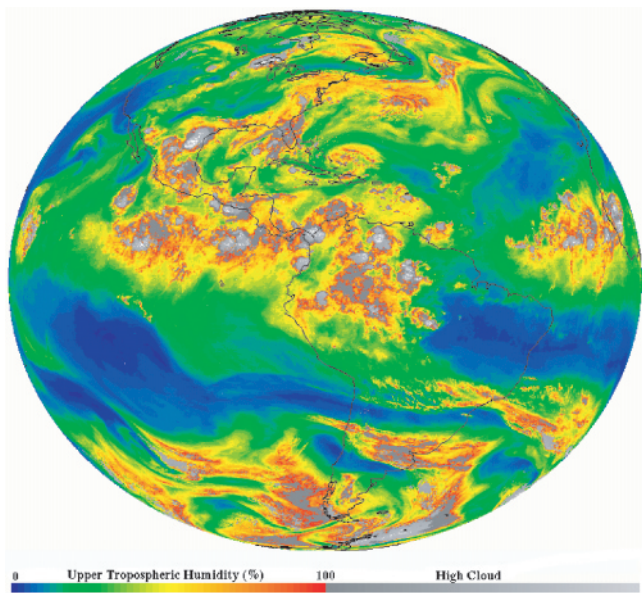


Figure 5 The upper tropospheric relative humidity (color) and cloud cover (grey) as observed from the Geostationary Operational Environmental Satellite (GOES-8) on April 27, 1999.

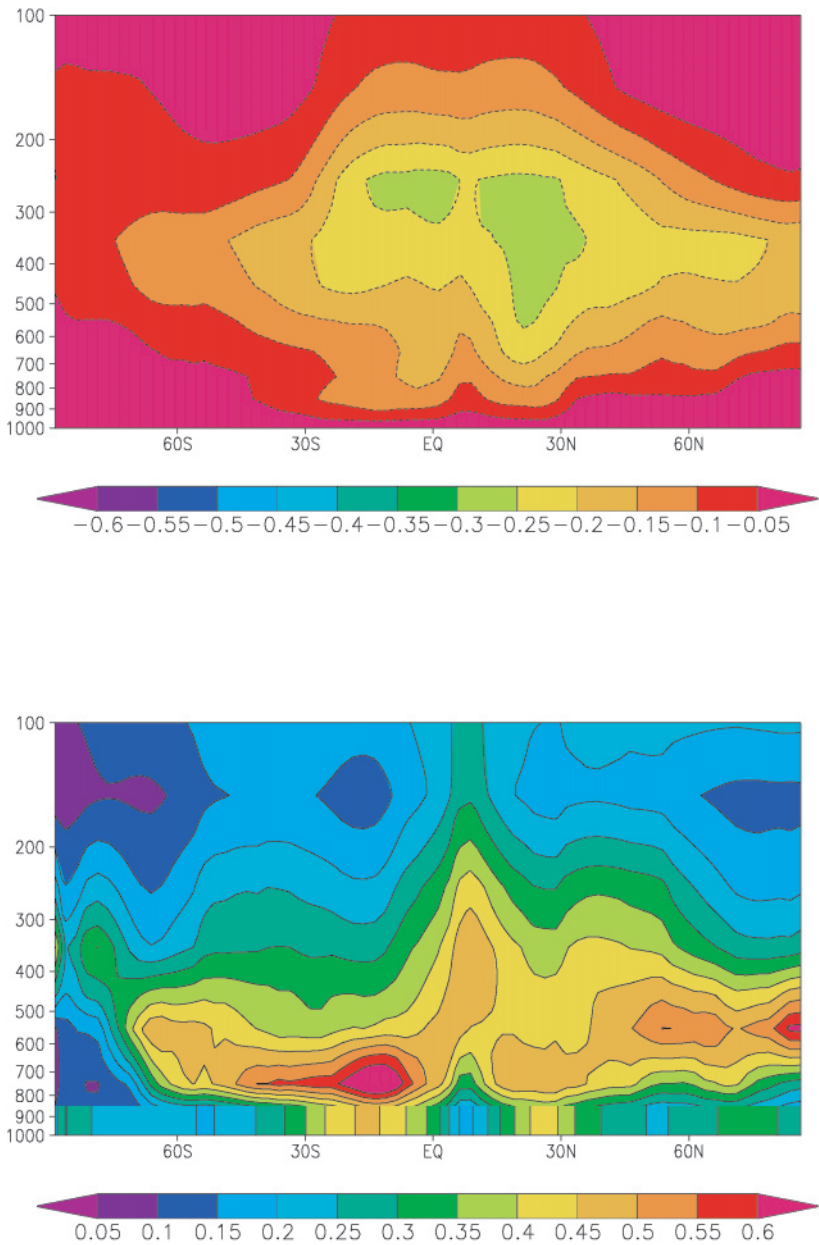


Figure 9 Height-latitude cross-sections of the sensitivity of the outgoing longwave radiation to perturbations in water vapor Q_e (*top*) and temperature Q_T (*bottom*) in 100 hPa thick layers. The results are expressed in units of $\text{Wm}^{-2}\text{K}^{-1}$.

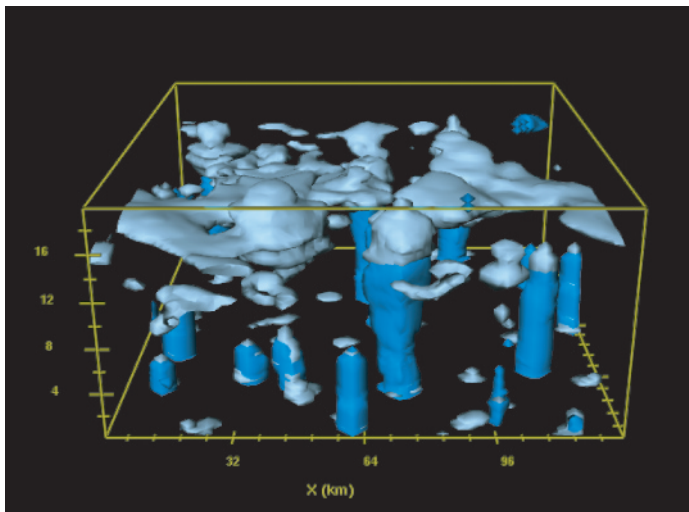


Figure 10 Distribution of cloud water (light blue) and precipitation (dark blue) simulated by the Geophysical Fluid Dynamics Laboratory resolved cloud model. Note the difference in scale between the regions of active convection with respect to a typical general circulation model grid box (yellow box).